Change detection in drill core images based on local binary pattern

__X. Gu__ [ID] ª, N.J. Cook ª, A.V. Metcalfe ᵇ and C. Aldrich ᶜ

ª School of Chemical Engineering, University of Adelaide, South Australia, Australia.
ᵇ School of Mathematical Sciences, University of Adelaide, South Australia, Australia.
ᶜ Western Australian School of Mines: Minerals, Energy and Chemical Engineering, Curtin University, WA, Australia
Email: xiaomeng.gu@adelaide.edu.au

Abstract: Demand for mineral resources is increasing, forcing mining companies to exploit lower grade and more heterogeneous ore bodies to maintain supply. High variability in mill feed leads to higher operating costs, greater energy and water usage, increased environmental impact, and in some cases, major capital investment to build more complex processing plants. Mining companies therefore need models that can accurately predict optimal processing parameters early in the life cycle of the mine, ideally from exploratory drill core data. Enhanced knowledge of ore body characteristics is vital for profitability and should ideally involve a geometallurgical program at the early stage of mine development that can help identify potential processing issues prior to major investment. Due to steady advances in technology, machine learning and the use of advanced statistics, much data is collected during exploration and resource drilling, yet this is often not used to its maximum to build robust geometallurgical models. Machine learning and deep learning are attracting research attention and implementation across the mining sector and fast becoming an integral part of industry's drive to greater agility and efficiency because they have the capacity to deal with large, multi-dimensional datasets.

The primary objective of this study is to employ Hotelling T^2 and squared prediction error (SPE) control charts to detect changes in optical images of drill core using latent variables extracted from the images' features. Local binary pattern (LBP) is utilized as the feature extraction method and has been previously validated as a robust and efficient technique for various mining applications. Results from a test drill hole suggest the presence of two main regimes separate mid-way along the drill core (at ca. 350m), and also show that LBP features are sensitive to the reference data used for constructing the control charts.

Keywords: *Local binary pattern, multivariate process control, image analysis, mineral processing*

1 INTRODUCTION

The exploitation of increasingly lower grade and more heterogeneous ore bodies is driving mining companies to acquire an enhanced knowledge of ore body characteristics in order to sustain profitability. Mineral textures play an important, yet often overlooked role in prediction of mineral processing behaviour and can be identified as a key geometallurgical indicator. Mineral textures have inextricable relationships with both lithology and mineralogy but are also linked to other ore properties such as porosity, the relationships between grains of different minerals, and the physical arrangement between ore and gangue components. This information is crucial for understanding, predicting, and hence optimising, downstream processes. Numerous authors have shown that rock texture affects strength, grindability, liberation, target grain size, and product particle size distributions in the comminution circuit. Texture also impacts potential mineral grade-recovery relationships during flotation (Gaspar & Pinto 1991). It is worth noting that even ores with identical chemical and mineral compositions can behave very differently during downstream processes if their textures differ substantially (Donskoi et al. 2016).

Drill core images are a crucial source of information for geologists, mineralogists, and mining engineers. These images capture the physical and chemical properties of the rock formations and provide valuable insights into the geological history of the region. However, the visual inspection of drill core images is often time-consuming and subjective, making it difficult to detect subtle changes in textural properties over time. Therefore, there is a growing need to develop automated and objective methods for change detection in drill core images.

2 MATERIALS AND METHODS

The drill core, which is 96 mm in diameter and 598.2 m in length, was obtained from the Boart Longyear test site at Brukunga, South Australia. One hundred and three optical images were taken using a 360° rotational camera, each being a rectangle of size 302 mm by 5800 mm, with a resolution of 144 dots per inch (psi). Each optical image consists of 170 by 1396 pixels. Examples of optical drill core images are shown in Figure 1. Artifacts can be observed on the images as black clouds and black vertical lines in the centre of the core. Each optical image was then divided into non-overlapping sub-images for textural analysis, each representing an interval roughly 0.1 m in length. We refer to these 5,982 sub-images as images. The local binary pattern (LBP) is calculated for each image, as a textural descriptor. Summary features of the LBPs are defined, and the aim is to use these features to identify outlying images or outlying segments of contiguous images.

Figure 1. Examples of optical drill core images, each of 5.8 m in depth.

2.1 Local binary pattern (LBP)

Local binary pattern (LBP) is a texture descriptor that captures the local variations in an image by comparing the intensity of a pixel to its neighbouring pixels. Mathematically, given the central pixel c, the LBP$r, p(c)$

Gu et al., Change detection in drill core images based on local binary pattern.

code at c with distance of r, and p neighbours is as follows:

$$LBPr, p(c) = \sum_{b=0}^{p-1} s(g_b - g_c)2^b, \qquad s(x) = \begin{cases} 1, & x \geq 0. \\ 0, & x < 0. \end{cases} \qquad (1)$$

where $g(.)$ represents the grey value, and r represents radius of circle and p is the associated number of neighbours. Typically, radius r is taken as 1 and gives p value of 8. An example is illustrated below (Figure 2).
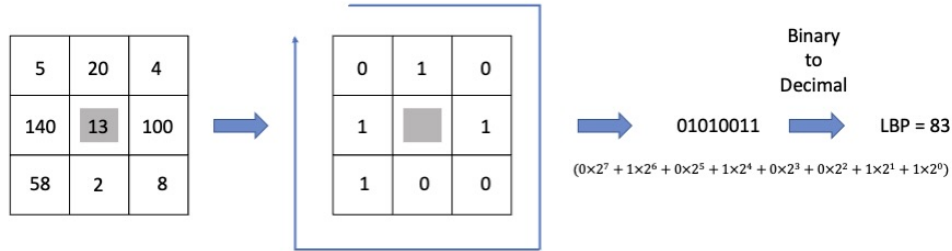

Figure 2. An example of calculating the $LBP_{1,8}()$, for the central cell with gray value of 13.

Local binary pattern (LBP) is straightforward to describe and implement, and has been applied widely. However, its high dimensional feature space makes it computationally expensive. Compared with the traditional LBP which considers all possible 2^8 sequences, uniform LBP gives a lower dimension of feature vector (59 features) and the idea is based on the assumption that some LBP features occur more frequently than others. Uniform LBP focuses on sequences of cells surrounding pixels that change from lighter than the central pixel to darker than the central pixel at most once (Figure 3). That is at most two 0-1 or 1-0 transitions, and all the other patterns are assigned to a single bin. The result is 58 uniform binary patterns and 1 non-uniform pattern, where the 58 features correspond to the following decimal LBP values: 0, 1, 2, 3, 4, 6, 7, 8, 12, 14, 15, 16, 24, 28, 30, 31, 32, 48, 56, 60, 62, 63, 64, 96, 112, 120, 124, 126, 127, 128, 129, 131, 135, 143, 159, 191, 192, 193, 195, 199, 207, 223, 224, 225, 227, 231, 239, 240, 241, 243, 247, 248, 249, 251, 252, 253, 254 and 255 (Figure 3). So, for each image with r rows and c columns, where r varies around 24 and c is 170, the LBP pattern is identified for non-edge pixels giving a $r - 2$ by $c - 2$ LBP matrix. A LBP histogram with 59 bins, corresponding to the count of each of the 59 uniform LBP patterns, is then built to represent the image. We define the counts as the image features (f_k).
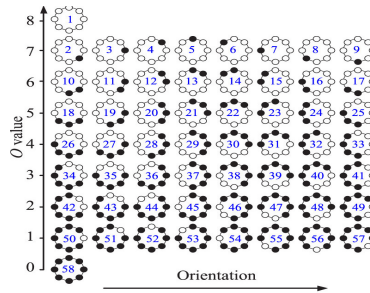

Figure 3. Uniform LBP patterns.

2.2 Change detection using LBP features

We have a sequence of 5,982 images, each consisting of 59 features, and we refer this sequence as a (multivariate) depth series. The principal component analysis (PCA) is implemented to reduce not only the dimension

of the features, but also eliminate the correlations between the features. The correlations of the 59 features are calculated, and form a 59×59 correlation matrix. The PCA follows directly from the eigenvalues and eigenvectors of the correlation matrix, that is

$$C = PDP^T,$$

where C is the correlation matrix, P consists of the eigenvectors and D is a diagonal matrix consisting of the eigenvalues. The first 20 principal components (PCs) are used, as they account more then 80% of the variability in the features, and have the form

$$\begin{bmatrix} PC_1 \\ \vdots \\ PC_{20} \end{bmatrix} = \begin{bmatrix} a_{1,1} & \ldots & a_{1,59} \\ \vdots & \vdots & \vdots \\ a_{20,1} & \ldots & a_{20,59} \end{bmatrix} \begin{bmatrix} f_1 \\ \vdots \\ f_{59} \end{bmatrix}$$

and variance λ_j, where λ_j is the eigenvalue for PC_j and $(a_{j,1}, \ldots a_{j,59})$ is the corresponding eigenvector. We define the value of PC_j for image i as t_{ij}, and the variance of PC_j is λ_j. Hotelling T^2 is defined as

$$T_i^2 = \sum_{j=1}^{20} \frac{t_{ij}^2}{\lambda_j}, \tag{2}$$

for $i = 1, \ldots, 5982$. Large values of T^2 identify outlying observations.

The squared prediction error (SPE) statistic is an alternative indicator of outlying values, and is calculated as follows. We define the features for image i as f_{ik} where k runs from 1 up to 59. We then project these 59 features onto the first 20 PCs, that is

$$\hat{f} = A^T PC \iff \begin{bmatrix} \hat{f}_1 \\ \vdots \\ \hat{f}_{59} \end{bmatrix} = \begin{bmatrix} a_{1,1} & \ldots & a_{1,59} \\ \vdots & \vdots & \vdots \\ a_{20,1} & \ldots & a_{20,59} \end{bmatrix}^\top \begin{bmatrix} PC_1 \\ \vdots \\ PC_{20} \end{bmatrix}.$$

Then,

$$SPE_i = \sum_{k=1}^{59} (f_{ik} - \hat{f}_{ik})^2, \text{ for } i = 1, \ldots, 5982. \tag{3}$$

The Hotelling T^2 and SPE statistics are commonly used in multivariate statistical process control (MVSPC), when it is assumed that the mean and covariance structure will be constant when the process is operating correctly. However, a constant mean and covariance structure is not realistic for a drill core. We can still formally implement MVSPC, using either the correlation matrix calculated from the entire length of the drill core or the correlation matrix based on a particular segment of the drill core (reference group). Here, we perform PCA of the features for: all 5,982 images in the entire depth series; and also for five sub-sequences of the images. To obtain the five reference groups, we divide 5,982 images into five consecutive non-overlapping groups (i.e, in the first group i runs from 1 up to 1,196, in the second group i runs from 1,197 to 2,392 and so on). A PCA model is then applied to each reference group, and used as the base for the Hotelling T^2 and SPE for the entire depth series. The rationale is that if the correlation matrix changes outside the reference group this will lead to increases in the levels of T^2 and SPE. For example with T^2, changes in PC_{20} which are relatively small in the reference group get divided by the relatively small λ_{20}, and if changes in PC_{20} tend to be larger outside the reference group they will have a substantial impact on T^2 when divided by the λ_{20} calculated from the reference group.

Both T_i^2 and SPE_i are plotted against image number, i, as is the custom for MVSPC. However, in MVSPC control limits are set from theory based on an assumption of independent observations from a multivariate normal distribution whereas we set empirical control limits as the upper 1% of the marginal distribution corresponding to the reference set. Furthermore, in the MVSPC setting, when the process is operating correctly, different reference sets are expected to give the same PCA. But, in the context of drill cores different reference sets may give substantially different PCAs. If different reference sets do give different PCAs, this is an indicator of differences between reference sets, and that could indicate differences in geometallurgical properties.
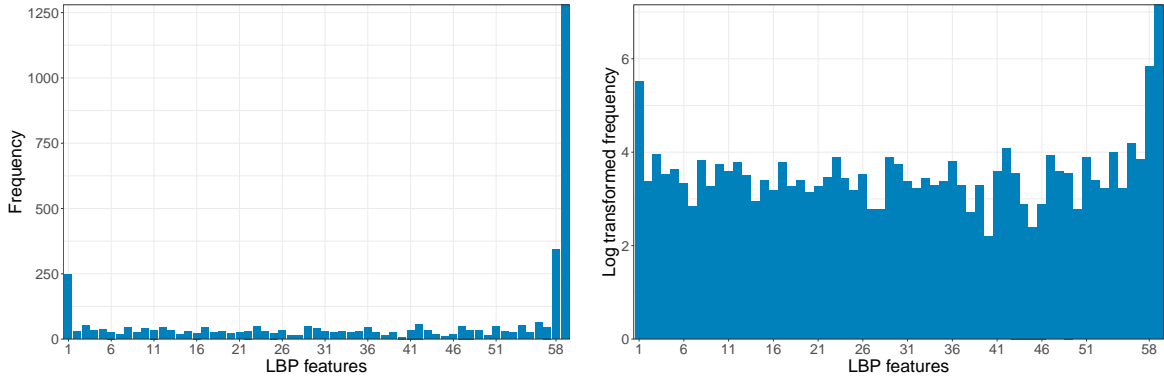
Gu et al., Change detection in drill core images based on local binary pattern.

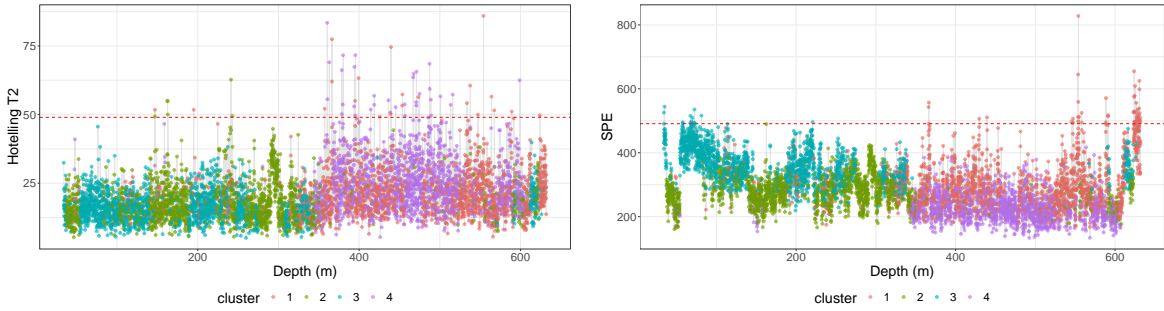**Figure 4**. Histogram of uniform LBP features (left) and log transformed (right).

Figure 5. Hotelling T^2 and SPE control charts with PCA model applied to all the images, coloured by different clusters.

3 RESULTS AND DISCUSSION

The log transformed uniform LBP features were used so as to eliminate the peak in the LBP histograms (non-uniform binary patterns), to avoid the other patterns category dominating the analysis. Also, the sum of the counts for an image is constrained to equal the number of pixels in that image and taking logarithms removes this linear constraint. Figure 4 is an example of a LBP histogram and log transformed LBP histogram. To provide a contrast to the depth series analysis which takes account of the ordering of the images, particularly when investigating the effects of different reference sets, we performed a K-means cluster analysis which is not influenced by the order of the images. K-means clustering was performed to the log transformed uniform LBP features with a chosen K value of 4. The number of clusters was determined based on elbow method, silhouette coefficient and visualisation of images in each cluster. As noted above, the clustering takes no account of the locations of the images along the drill core. The next stage in the analysis is to identify different segments of drill core such that contiguous images in a segment are relatively similar and substantially different from those in neighbouring segments.

A PCA model has been applied to the features of all the images, and the control charts are constructed based on the first 20 PCs (Figure 5). Both of the Hotelling T^2 and SPE control charts suggest a shift in the mean values around 350 meters, and SPE control chart also shows slight "w" shape in the first half of the drill core.

To assess the sensitivity of the use of the reference group, a PCA model was fitted to each reference group. The first 20 PCs were used to construct the control charts, colored by the 4 clusters (Figure 6). The upper 99% quantile of the reference group was used as upper control limit, and is shown as red dashed line in the control charts.

The control charts for the second half of the drill core appear concave (Figure 6a, Figure 6c and Figure 6d) when using group 1 and 2 as reference data. However, this concavity was not evident in the SPE control chart when group 1 was used as reference (Figure 6b). Notably, the control charts indicated the presence of two distinct regimes that separated roughly mid-way along the drill core, a finding that was also supported by the
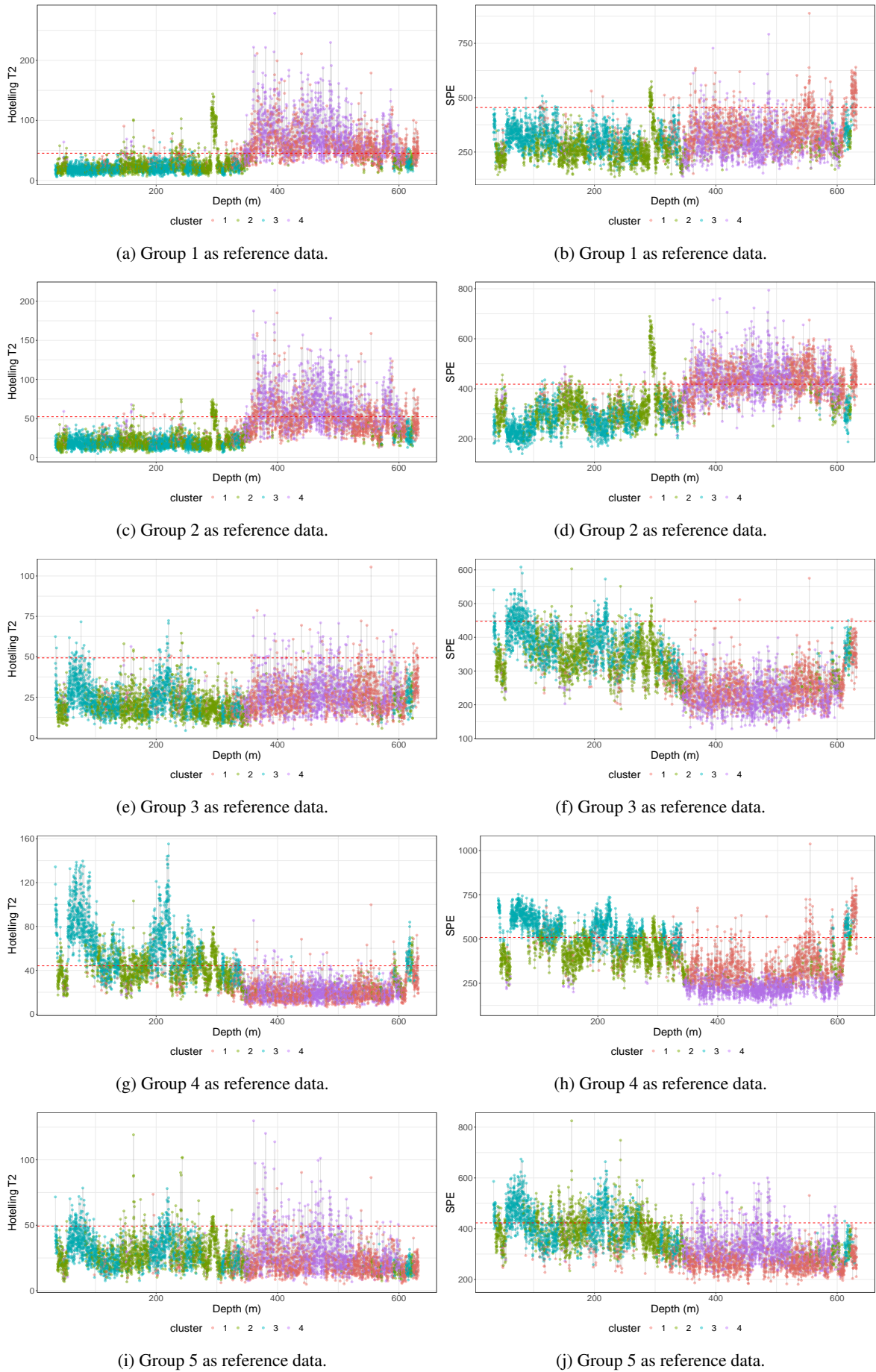
(a) Group 1 as reference data.

(b) Group 1 as reference data.

(c) Group 2 as reference data.

(d) Group 2 as reference data.

(e) Group 3 as reference data.

(f) Group 3 as reference data.

(g) Group 4 as reference data.

(h) Group 4 as reference data.

(i) Group 5 as reference data.

(j) Group 5 as reference data.

Figure 6. Hotelling T^2 and SPE statistics calculated using log transformed uniform LBP features, with different groups as reference, coloured by 4 different clusters.

clustering analysis. When group 3 was used as reference data, the Hotelling T^2 control chart was relatively stable (Figure 6e), but the SPE control chart revealed curvatures in both the first and second half of the drill core (Figure 6f), with the first half exhibiting a "w" shape that suggested a change in the first quarter. Similarly, both the Hotelling T^2 and SPE control charts indicated changes in texture every quarter along the drill core in Figure 6g and Figure 6h when group 4 was used as reference. In contrast, the control charts for group 5 as reference data were not informative. The conclusions drawn from these observations were supported by Table 1, which showed that the number of out-of-control images varied depending on the group used as reference data, with groups 3 and 5 displaying relatively fewer out-of-control images compared to the other three groups. Furthermore, it is worth noting that the SPE control chart, when using group 4 as a reference, displays more outlying values compared to the Hotelling T^2 control chart.

Table 1. Number of out-of-control observations for Hotelling T^2 and SPE control charts, with different renference data for PCA model.

	Hotelling T^2	SPE	Both					
			Group 1	Group 2	Group 3	Group 4	Group 5	Total
Group 1	2209	280	0	3	62	47	104	216
Group 2	1375	1801	0	1	233	575	273	1082
Group 3	131	262	15	13	1	1	2	32
Group 4	1741	1597	645	389	95	3	86	1218
Group 5	292	1177	58	70	24	50	5	207

Based on the results presented in Table 1, it is evident that the number of outlying images varies for different reference data groups. Notably, the use of group 1 or 2 as reference data resulted in the absence of any outlying images in group 1 detected by both control charts. Furthermore, the fewest outlying images were detected when using group 3 as the reference data, indicating that this group has relatively higher PC scores compared to the other groups. When using group 4 or 5 as reference data, a higher number of outlying images were detected in group 1 and group 2 by both control charts. These findings suggest the presence of two regimes that are separated by the midpoint of the drill core.

4 CONCLUSION

Overall, the control charts demonstrate substantial differences depending on the group used as reference data, indicating changes in textural properties, particularly between the upper and lower halves of the drill core, but, to a lesser degree, also at 190 m and 480 m.

There is no theoretical bases for the choice of using the first 20 PCs and five reference groups, and this could be varied. Nevertheless, the results of this study provide a foundation for further research to explore the use of gray-level co-occurrence matrix (GLCM) and convolutional neural networks (CNNs) for detecting changes in drill core images, as they have also been shown to be effective in similar applications. A comparison between LBP, GLCM, and CNN approaches provides valuable insights into the performance of each method and their suitability for different types of image analysis tasks.

REFERENCES

Donskoi, E., Poliakov, A., Holmes, R., Suthers, S., Ware, N., Manuel, J. & Clout, J. (2016), 'Iron ore textural information is the key for prediction of downstream process performance', *Minerals Engineering* **86**, 10–23.

Gaspar, O. & Pinto, A. (1991), 'The ore textures of the neves-corvo volcanogenic massive sulphides and their implications for ore beneficiation', *Mineralogical Magazine* **55**(380), 417–422.